ChemComm

Accepted Manuscript

This article can be cited before page numbers have been issued, to do this please use: J. Wu, J. Tian, L. Rui and W. Zhang, *Chem. Commun.*, 2018, DOI: 10.1039/C8CC04275F.

ROYAL SOCIETY OF CHEMISTRY

rsc.li/chemcomm

View Article Online
DOI: 10.1039/C8CC04275F

Journal Name

COMMUNICATION

Enhancing the efficacy of photodynamic therapy (PDT) *via* water-soluble pillar[5]arene-based supramolecular complexes

Received 00th January 20xx,
Accepted 00th January 20xx

DOI: 10.1039/x0xx00000x

www.rsc.org/

Jian Wu, Jia Tian, Leilei Rui, Weian Zhang*

A supramolecular nanovesicle was constructed by the complexation between pyrophaeophorbide A (PPhA) and water-soluble pillar[5]arene, then a biotin-pyridinium targeting agent was introduced to its surface. The nanovesicle exhibited reduced aggregation of PPhA photosensitizers and high targeting ability towards cancer cells, therefore leading to excellent therapeutic efficacy under red light.

Photodynamic therapy (PDT) has emerged as a promising treatment for cancers due to its unique advantages of minimal invasiveness, high spatiotemporal accuracy and low side effects[1]. PDT involves the administration of photosensitizers (PSs) and a specific wavelength of light to generate reactive oxygen species (ROS), including singlet oxygen ($^1O_2$) which could irreversibly damage tumour tissues[2]. In the process of PDT, photosensitizer plays a critical role in producing highly reactive singlet oxygen. Therefore, the selection of efficient PSs is of utmost importance. However, conventional clinically used PSs are hydrophobic and greatly aggregated in aqueous solution, which severely limit clinic potential of PDT[3]. To surmount these issues, Na *et al*. developed natural polymer-based nanocarriers to increase PSs solubility in aqueous solution, and Zhang *et al*. used polypeptide to improve PSs selectivity[4]. In comparison with the improving water solubility of PSs, there is no more attention on another big challenge in PDT, i. e., aggregation of PSs *via* stacking, resulting in low singlet oxygen production and unsatisfactory PDT efficacy[5]. To decrease the aggregation and improve singlet oxygen yield, some strategies have been adopted, including constructing PS-based metal-organic frameworks (MOF), and introducing bulky groups onto the PS macrocycles. For instance, Lin *et al.* developed PS-based nanoscale metal-organic framework (NMOF) for efficient ROS generation[6]. Hu *et al.* also fabricated a human serum albumin-based core-shell nanostructure to prevent self-quenching of PSs[7].

Supramolecular chemistry based on host-guest interaction has undergone rapid development over the past few decades[8]. Benefiting from the host-guest recognition, functional supramolecular systems can be fabricated by using macrocycle compounds such as cyclodextrins, cucurbit[*n*]urils, calix[*n*]arenes and pillar[*n*]arenes[9]. Among them, cyclodextrin-based host-guest supramolecular complexes have been widely utilized in biomedicine field[10]. For example, Strassert and his co-workers developed cyclodextrin vesicles to reduce aggregation of phthalocyanine in aqueous solution[5]. Cucurbit[8]uril and calix[4]arene derivatives were also designed as supramolecular drug delivery system (DDS) for cancer therapy[9]. More recently, pillar[*n*]arenes, mainly including pillar[5]arenes and pillar[6]arenes, have been widely studied because of their symmetrical pillar architectures, electron-donating cavities and easy functionalization[11]. Among them, water-soluble pillar[*n*]arenes has caught much attention because of their good biocompatibility and water solubility[13]. Therefore, employing water-soluble pillar[*n*]arene-based recognition motif to construct supramolecular DDS is of great interest[12]. Huang *et al.* developed pillar[5]arene-based supramolecular amphiphiles for controlled release of DOX[13]. Wang *et al*. also constructed supramolecular nanoparticles in application of rapid drug release[14]. However, there are few reports on the application of water-soluble pillar[*n*]arenes-based supramolecular complexes in PDT[12]. Furthermore, photodynamic activity of PSs enhanced by water-soluble pillar[5]arenes has not been reported yet.

Herein, we designed a host-guest supramolecular system constructed by pyrophaeophorbide A-pyridinium (PPhA-Py) and water-soluble pillar[5]arene (P[5]A). P[5]A was utilized to improve water solubility and suppressed aggregation of PPhA through host-guest interaction. Thus, this recognition motif was able to form stable vesicle with enhanced fluorescence and singlet oxygen production in water. Furthermore,

Shanghai Key Laboratory of Functional Materials Chemistry, Key Laboratory for Specially Functional Polymeric Materials and Related Technology of the Ministry of Education, East China University of Science and Technology, 130 Meilong Road, Shanghai 200237, China
Email: wazhang@ecust.edu.cn (W. Zhang);
Tel/Fax.: +86 21 64253033
Electronic Supplementary Information (ESI) available: [details of any supplementary information available should be included here]. See DOI: 10.1039/x0xx00000x

View Article Online
DOI: 10.1039/C8CC04275F

targeting agent biotin-pyridinium (Bt-Py) was decorated on the surface of P[5]A/PPhA-Py vesicle with the aim of improving cellular uptake of PSs (**Scheme 1**). The phototoxicity of PS against HeLa cells was evaluated by MTT assay to measure PDT effect. This supramolecular PS may indeed promote cancer PDT treatment with great potential for clinic treatment.

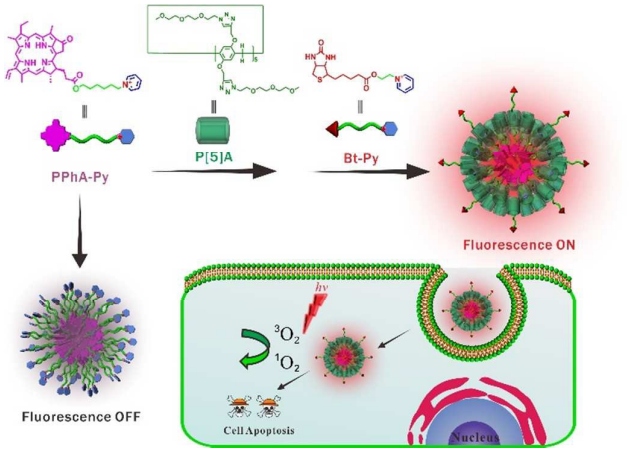

Scheme 1 Illustration of enhanced fluorescence of P[5]A/PPhA-Py, and therapeutic effect of P[5]A/PPhA-Py/Bt-Py in cancer cells.

The synthetic methods of P[5]A, PPhA-Py, Bt-Py and model guest (G_M) were shown in Supporting Information (**Scheme S1-S4**). Before constructing supramolecular photosensitizers P[5]A/PPhA-Py, we first investigated the complexation between P[5]A and pyridinium moiety by ^{1}H NMR spectroscopy in D_2O. Owing to the poor water solubility of PPhA-Py, a model guest G_M was used in NMR titration. As shown in **Fig. 1A**, resonance peaks of protons H_a, H_c and H_e on P[5]A shifted downfield slightly upon addition of G_M. On the other hand, slight upfield shifts were observed for H_4, H_5, H_6 and H_7 protons of G_M because of shielding effect of the electron-rich cavities of P[5]A. Moreover, the signal of proton H_3 on pyridine ring disappeared owing to broadening effect[16]. Additionally, ^{1}H NMR titration experiment between PPhA-Py and P[5]A was also performed in $CDCl_3$, which is similar to that between G_M and P[5]A in D_2O (**Fig. S8**). From 2D NOESY spectrum, intermolecular correlations were also observed between proton H_c on the P[5]A and protons H_2, H_6 on G_M (**Fig. S9**). These phenomena clearly demonstrated the inclusion complexation occurred between P[5]A and pyridinium moiety in aqueous solution.

Fluorescence titration experiment was further used to determine the association constant (K_a) between P[5]A and PPhA-Py in aqueous solution (**Fig. 1B**). We studied fluorescence spectra of increasingly concentrated solution of P[5]A at constant concentration of PPhA-Py. Obviously, a remarkable enhancement of fluorescence at 685 nm for increasing concentration of P[5]A was observed, reaching a maximum at a P[5]A concentration of 0.12 mM. Whereas, no significant fluorescence signal was obtained from the solution of free PPhA-Py. Therefore, we assumed that ACQ of PPhA-Py was effectively prevented by P[5]A. Besides, the association constant (K_a) was calculated to be (1.91 ± 0.58) × 10^4 M^{-1} (**Fig. 1C**) by non-linear curve-fitting method based on fluorescence experiments. Job's plot method had also been used to study the stoichiometry complexation between P[5]A and PPhA-Py in aqueous solution, which revealed a 1:1 stoichiometric ratio (**Fig. S10**).

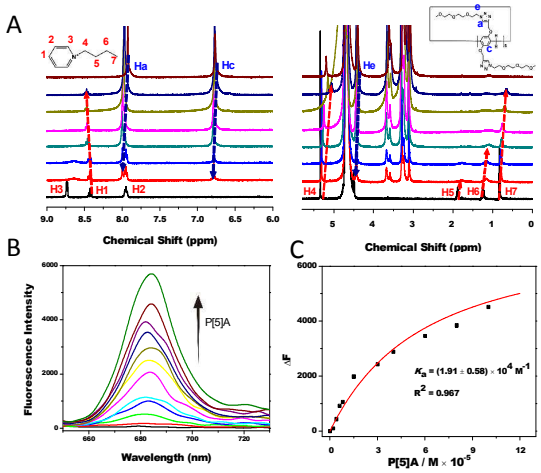

Fig. 1 (A) Partial ^{1}H NMR spectra (400 MHz, D_2O) of G_M at a constant concentration of 2 mM with different concentrations of P[5]A: (a) 0.0, (b) 0.5, (c) 1.0, (d) 1.5, (e) 2.0, (f) 3.0, (g) 4.0 and (h) individual P[5]A (2.00 mM). (B) Fluorescence spectra of PPhA-Py (1.0 × 10^{-5} M) in aqueous solution with different concentrations of P[5]A: 0, 0.2, 0.4, 0.6, 0.8, 1.5, 3.0, 4.0, 6.0, 8.0, 10.0, and 12 × 10^{-5} M. (C) The fluorescence intensity changes upon addition of P[5]A. The red solid line was obtained from the non-linear curve-fitting.

Further evidence for the inclusion between P[5]A and PPhA-Py was provided by UV-*vis* absorption spectroscopy. As shown in **Fig. S11**, the mixture solution of P[5]A and PPhA-Py exhibited strong absorption at 300 nm and 400 nm in aqueous media, corresponding to the typical absorption of P[5]A and PPhA-Py, respectively. Notably, the Soret-band of PPhA-Py had a slight red shift from 400 nm to 425 nm, demonstrating the occurrence of host-guest complexation.

The stable supramolecular aggregates were fabricated by reprecipitation method. Firstly, P[5]A/PPhA-Py (molar ratio, 3/1) DMF solution was added dropwise into deionized water with stirring, then the mixture solution was dialyzed against deionized water for removing DMF. A similar procedure was also utilized to construct stable PPhA-Py assemblies. In order to study the self-assembly behaviour of P[5]A/PPhA-Py complexes, pyrene was used as a fluorescence probe to measure the critical vesicle concentration (CVC), and the CVC value was determined to be 5.5 × 10^{-3} mg mL^{-1} in aqueous solution as shown in **Fig. S12**.

The morphology and size of these assemblies were further investigated by TEM and DLS. Obviously, TEM image showed spherical morphologies of PPhA-Py assemblies with diameters of about 150 nm (**Fig. 2A**). In **Fig. 2B**, spherical vesicles with diameters of about 120 nm were clearly observed in the TEM

View Article Online
DOI: 10.1039/C8CC04275F

image which was smaller than DLS result (average size of 165 nm, **Fig. S13**). The formation of spherical vesicles was mainly driven by the host-guest interaction and the amphiphilicity of supramolecular complexes.

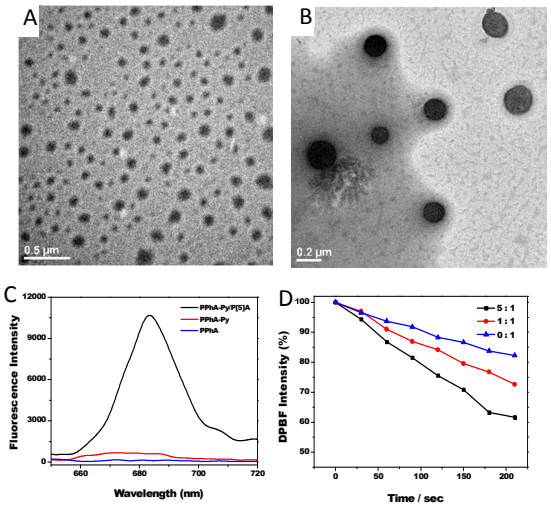

Fig. 2 TEM images: (A) PPhA-Py spherical nanoparticles; (B) P[5]A/PPhA-Py supramolecular nanoparticles. (C) Fluorescence spectra of PPhA, PPhA-Py and P[5]A/PPhA-Py in aqueous solution at room temperature. (D) DPBF degradation rate in different solution, blue line: P[5]A:PPhA = 0:1; red line: P[5]A:PPhA = 1:1 and black line: P[5]A:PPhA = 5:1.

As expected, P[5]A/PPhA-Py vesicles showed enhanced fluorescence in contrast to free PPhA and PPhA-Py aggregates in aqueous solution (**Fig. 2C**). We speculated that the host-guest interaction of pyridinium moiety with the cavity of P[5]A compensated the free energy of aggregation. The host-guest interaction driven by electrostatic force overcame the stacking effect of PPhA-Py, a process that was driven by hydrophobic exclusion of porphine rings[3].

The generation of singlet oxygen was chemically detected by 1, 3-diphenylisobenzofuran (DPBF) in a DMF/H_2O (1:100, v/v) mixed solution[17]. The decay of DPBF at 450 nm was monitored every 30 s under a 660 nm laser light. **Fig. S14** showed the UV absorption of DPBF after reacting with $^1O_2$ produced by PPhA under different irradiation time. The absorption of DPBF at 450 nm was plotted against irradiation time for P[5]A/PPhA-Py solutions (molar ratio, 5:1 and 1:1) and free PPhA-Py solution, as shown in **Fig. 2D**. We can clearly notice that less DPBF was decomposed in free PPhA-Py solution after exposed to 660 nm laser light, indicating there were no more $^1O_2$ generated from free PPhA-Py in in aqueous medium. Surprisingly, much more $^1O_2$ was produced from P[5]A/PPhA-Py solutions, as less DPBF was remained after irradiation. Moreover, P[5]A/PPhA-Py at a molar ratio of 5:1 had much higher $^1O_2$ yield than that of 1:1, demonstrating the introduction of WP5 could greatly reduce the aggregation of PPhA and improve $^1O_2$ generation by the formation of P[5]A/PPhA-Py complexes.

Cellular uptake of P[5]A/PPhA-Py complexes was investigated by flow cytometry and confocal laser scanning microscopy (CLSM), respectively. To improve the cellular uptake and reduce potential cytotoxicity of P[5]A/PPhA-Py supramolecular complexes, targeting moieties biotin-pyridinium were introduced to form P[5]A/PPhA-Py/Bt-Py vesicles through host-guest interaction. The tracked results of free PPhA, PPhA-Py assemblies, P[5]A/PPhA-Py vesicles and P[5]A/PPhA-Py/Bt-Py vesicles were quantitatively analyzed by flow cytometry as illustrated in **Fig. S15**. After 4 h of co-incubation, four samples were taken up by HeLa cells as their fluorescence curves moved to the right of control group. When the incubation time was prolonged to 24 h, stronger fluorescence can be clearly observed for all groups, suggesting the time-dependent cellular uptake behaviour. Besides, the enhanced cellular uptake of P[5]A/PPhA-Py vesicles compared with free PPhA and PPhA-Py assemblies may be that P[5]A/PPhA-Py vesicles were taken up by cells *via* endocytosis process, while free PPhA and PPhA-Py assemblies was transported *via* passive diffusion. Moreover, cells treated with P[5]A/PPhA-Py/Bt-Py vesicles displayed strongest fluorescence both in 4h and 24 h, indicating excellent targeting ability of biotin towards HeLa cells.

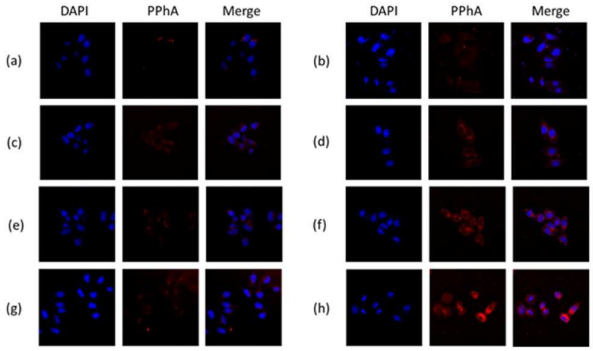

Fig. 3 CLSM images of HeLa cells incubated with different samples : (a) PPhA for 4 h, (b) PPhA for 24 h, (c) PPhA-Py assemblies for 4 h, (d) PPhA-Py assemblies for 24 h, (e) P[5]A/PPhA-Py supramolecular vesicles for 4 h, (f) P[5]A/PPhA-Py supramolecular vesicles for 24 h, (g) P[5]A/PPhA-Py/Bt-Py supramolecular vesicles for 4 h, (h) P[5]A/PPhA-Py/Bt-Py supramolecular vesicles for 24 h.

CLSM was further conducted to investigate the cellular uptake behaviour. As shown in **Fig. 3**, 4, 6-diamidino-2-phenylindole (DAPI) with blue fluorescence was used to stain the nucleus to locate the predetermined cells. Meanwhile, the red fluorescence of PPhA was mainly found in cytoplasm and became brighter in the cells when incubation time prolonged to 24 h. Notably, P[5]A/PPhA-Py vesicles showed relatively stronger fluorescence than PPhA-Py assemblies and free PPhA. Furthermore, the strongest fluorescence was observed for groups of cells treated with P[5]A/PPhA-Py/Bt-Py vesicles which was in good agreement with the flow cytometry results.

Finally, the dark cytotoxicity and phototoxicity of nanoparticles against HeLa cells were separately evaluated by MTT assy. As shown in **Fig. 4A**, it could be seen that group for free PPhA showed obvious cytotoxicity with a cell viability of 81%, when the concentration of free PPhA increased to 5 μg

View Article Online
DOI: 10.1039/C8CC04275F

mL^{-1}. However, PPhA-Py assemblies, P[5]A/PPhA-Py vesicles and P[5]A/PPhA-Py/Bt-Py vesicles at concentration ranging from 0.04 μg mL^{-1} to 5 μg mL^{-1} (calculated for PPhA concentration) did not cause obvious dark cytotoxicity after 24 h incubation compared with the control group, which indicated the formation of assemblies could effectively decrease the dark cytotoxicity of free PPhA.

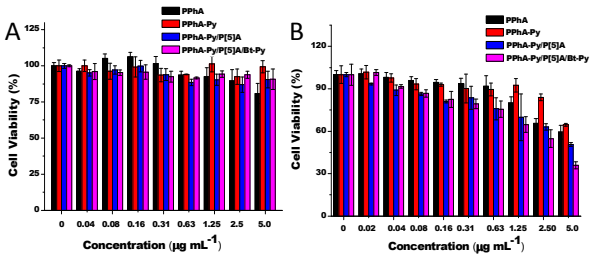

Fig.4 In vitro dark cytotoxicity (A) and phototoxicity (B) of free PPhA, PPhA-Py assemblies, P[5]A/PPhA-Py supramolecular vesicles and P[5]A/PPhA-Py/Bt-Py supramolecular vesicles against HeLa cells.

For the phototoxicity, after 20 min light irradiation, all groups exhibited significant PSs concentration-dependent cytotoxicity towards HeLa cells (**Fig. 4B**). It was notable that P[5]A/PPhA-Py vesicles led to higher cell mortality rate compared with free PPhA and PPhA-Py assemblies, indicating that PDT activity of PPhA had been effectively improved by water-soluble P[5]A *via* the formation of host-guest complexes. Moreover, P[5]A/PPhA-Py/Bt-Py vesicles showed highest phototoxicity among four groups with an IC50 of 3.5 μg mL^{-1} (calculated for PPhA concentration) which was largely attributed to improved $^1O_2$ generation capability of PSs and their excellent targeting ability towards HeLa cells. As a consequence, P[5]A/PPhA-Py/Bt-Py vesicles could serve as ideal supramolecular PSs because of their negligible dark cytotoxicity, significant phototoxicity and excellent targeting ability.

In conclusion, we developed a novel supramolecular PS with improved $^1O_2$ production for enhancing the efficacy of PDT. In this supramolecular system, water-soluble P[5]A was first applied to suppress the aggregation of PSs and targeting agent biotin was introduced to improve the cellular uptake of PSs. The higher fluorescence intensity and singlet oxygen production of P[5]A/PPhA-Py assemblies clearly demonstrated the aggregation of PPhA-Py could be effectively inhibited by the formation of host-guest complexes between P[5]A and PPhA-Py. Furthermore, the introduction of targeting biotin for P[5]A/PPhA-Py complexes could increase cellar uptake of PSs, and further enhance the efficacy of PDT. Thus, this water-soluble P[5]A-based supramolecular system would provide a strategy for enhancing the efficacy of PDT.

Acknowledge

This work was financially supported by the National Natural Science Foundation of China (No. 21574039), and the Fundamental Research Funds for the Central Universities (222201814018).

Notes and references

1 Lucky, S. S.; Soo, K. C.; Zhang, Y. *Chem. Rev.*, **2015**, *115*, 1990.
2 Fan, W.; Huang, P.; Chen, X. *Chem. Soc. Rev.*, **2016**, *45*, 6488.
3 (a) Voskuhl, J.; Kauscher, U.; Gruener, M.; Frisch, H.; Wibbeling, B.; Strassert, C. A.; Ravoo, B. J. *Soft Matter*, **2013**, *9*, 2453. (b) Ethirajan, M.; Chen, Y.; Joshi, P.; Pandey, R. K. *Chem. Soc. Rev.*, **2011**, *40*, 340. (c) Zhou, Z.; Song, J.; Nie, L.; Chen, X. *Chem. Soc. Rev.*, **2016**, *45*, 6597.
4 (a) Kim, K. S.; Kim, J.; Lee, J. Y.; Matsuda, S.; Hideshima, S.; Mori, Y.; Osaka, T.; Na, K. *Nanoscale*, **2016**, *8*, 11625. (b) Qin, S.-Y.; Peng, M.-Y.; Rong, L.; Jia, H.-Z.; Chen, S.; Cheng, S.-X.; Feng, J.; Zhang, X.-Z. *Nanoscale*, **2015**, *7*, 14786.
5 Galstyan, A.; Kauscher, U.; Block, D.; Ravoo, B. J.; Strassert, C. A. *ACS Appl. Mater. Interfaces*, **2016**, *8*, 12631.
6 Lu, K.; He, C.; Lin, W. *J. Am. Chem. Soc.*, **2015**, *137*, 7600.
7 Ren, H.; Liu, J.; Su, F.; Ge, S.; Yuan, A.; Dai, W.; Wu, J.; Hu, Y. *ACS Appl. Mater. Interfaces*, **2017**, *9*, 3463.
8 (a) Liu, Z.; Nalluri, S. K. M.; Stoddart, J. F. *Chem. Soc. Rev.*, **2017**, *46*, 2459. (b) Guo, S.; Liang, T.; Song, Y.; Cheng, M.; Hu, X.-Y.; Zhu, J.-J.; Wang, L. *Polym. Chem.*, **2017**, *8*, 5718.
9 (a) Tong, H.; Du, J.; Li, H.; Jin, Q.; Wang, Y.; Ji, J. *Chem. Commun.*, **2016**, *52*, 11935. (b) Wang, Y.; Li, D.; Wang, H.; Chen, Y.; Han, H.; Jin, Q.; Ji, J. *Chem. Commun.*, **2014**, *50*, 9390. (c) Tu, C.; Zhu, L.; Li, P.; Chen, Y.; Su, Y.; Yan, D.; Zhu, X.; Zhou, G. *Chem. Commun.*, **2011**, *47*, 6063. (d) Zhou, J.; Yu, G.; Huang, F. *Chem. Soc. Rev.*, **2017**, *46*, 7021.
10 (a) Yasen, W.; Dong, R.; Zhou, L.; Huang, Y.; Guo, D.; Chen, D.; Li, C.; Aini, A.; Zhu, X. *Chem. Commun.*, 2017, *53*, 12782. (b) Dong, R.; Ravinathan, S. P.; Xue, L.; Li, N.; Zhang, Y.; Zhou, L.; Cao, C.; Zhu, X. *Chem. Commun.*, **2016**, *52*, 7950. (c) Yasen, W.; Dong, R.; Zhou, L.; Wu, J.; Cao, C.; Aini, A.; Zhu, X. *ACS Appl. Mater. Interfaces*, **2017**, *9*, 9006.
11 (a) Guo, S.; Liang, T.; Song, Y.; Cheng, M.; Hu, X.-Y.; Zhu, J.-J.; Wang, L. *Polym. Chem.*, **2017**, *8*, 5718. (b) Chen, J. F.; Lin, Q.; Zhang, Y. M.; Yao, H.; Wei, T. B. *Chem. Commun.*, 2017, *53*, 13296. (c) Lin, Q.; Zhong, K.-P.; Zhu, J.-H.; Ding, L.; Su, J.-X.; Yao, H.; Wei, T.-B.; Zhang, Y.-M. *Macromolecules*, **2017**, *50*, 7863.
12 (a) Yao, Y.; Chi, X.; Zhou, Y.; Huang, F. *Chem. Sci.*, **2014**, *5*, 2778. (b) Rui, L.; Xue, Y.; Wang, Y.; Gao, Y.; Zhang, W. *Chem. Commun.*, **2017**, *53*, 3126. (c) Zhang, Y.-M.; Zhu, W.; Qu, W.-J.; Zhong, K.-P.; Chen, X.-P.; Yao, H.; Wei, T.-B.; Lin, Q. *Chem. Commun.*, **2018**, *54*, 4549.
13 Zhou, Y.; Jie, K.; Huang, F. *Chem. Commun.*, **2017**, *53*, 8364.
14 Cao, Y.; Li, Y.; Hu, X.-Y.; Zou, X.; Xiong, S.; Lin, C.; Wang, L. *Chem. Mater.*, **2015**, *27*, 1110.
15 Chen, Y.; Rui, L.; Liu, L.; Zhang, W. *Polym. Chem.*, **2016**, *7*, 3268.
16 Laggoune, N.; Delattre, F.; Lyskawa, J.; Stoffelbach, F.; Guigner, J. M.; Ruellan, S.; Cooke, G.; Woisel, P. *Polym. Chem.*, **2015**, *6*, 7389.
17 Liu, G.; Qin, H.; Amano, T.; Murakami, T.; Komatsu, N. *ACS Appl. Mater. Interfaces*, **2015**, *7*, 23402.